SIMULATION STUDIES OF SRF CW PHOTOINJECTOR BRIGHTNESS OPTIMIZATION FOR DIFFERENT RF GUN GRADIENTS AND PHOTOCATHODE LASER PULSE SHAPES*

S. Zeeshan†, M. Krasilnikov, X. Li, Deutsches Elektronen Synchrotron DESY, Zeuthen, Germany

D. Bazyl, I. Zagorodnov, Deutsches Elektronen Synchrotron DESY, Hamburg, Germany

Abstract

Developments of a superconducting radiofrequency (SRF) photoinjector for future continuous-wave (CW) operation of the European XFEL are currently underway at DESY. A superconducting L-band 1.6-cell cavity is considered as a high brightness electron source capable of supporting CW operation and meeting the stringent beam quality requirements of cutting edge XFEL facilities. Given the limitations on the attainable gradient in the superconducting gun, photocathode laser pulse shaping provides an effective means of mitigating space charge driven emittance growth. In this study, 4D integral brightness; combining emittance and current profile is used as the main optimization objective. Multiobjective optimization using ASTRA has been performed to minimize the electron beam emittance and maximize its brightness for various temporal and transverse profiles of the photocathode laser pulse in the European XFEL SRF photo injector. Photocathode laser temporal and transverse distributions are compared in terms of achievable 4D beam brightness and their dependence on the attainable RF gradient in the SRF gun. The optimized photo injector working points are propagated through start-to-end simulations to evaluate brightness preservation up to the undulator entrance.

INTRODUCTION

The short wavelength FELs (European XFEL and FLASH) generate high brilliance coherent laser light and require high brightness electron beams [1][2]. To increase the average brilliance even further, the CW operation of photoinjector of the FELs is desired. For the EuXFEL the CW operation is under considerations since many years [3]. The proposed injector for the CW operation will use superconducting L-band 1.6 cell cavity [4]. The injector has been studied in detail including start-to-end simulation calculations for the beam transport to the undulators and FEL simulations on the X-ray intensities for the attainable photon energies [5]. The CW photoinjector layout has been modified later in terms of position of solenoid and the first accelerating cryomodule (A1) guided by the optimization of the photoinjector for the temporal flattop profile of the photocathode laser pulse.

The performance of the SRF photoinjector critically determines the XFEL beam quality and can put constraint in gaining the expected XFEL performance. Advanced shaping of the photocathode laser pulses, both temporaly and transversely, is essential to minimize emittance and maximize brightness, especially given the limited gun gradient and solenoid separation. The longitudinal Gaussian (G) with transverse radial uniform (RU) serves as a basic reference case. This is compared with more advance shapes like longitudinal flattop (FT) with transverse truncated Gaussian (TG) (1σ) which is identified as the most promising candidate for low emittance performance. The longitudinal FT with transverse RU represents a reasonable startup scenario while longitudinal Inverted parabolic (IP) with transverse TG can be considered as a feasible alternative to FTTG. In this study, these laser distributions and RF gradients in the SRF gun are systematically studied to identify optimal operating conditions and to evaluate the tolerance to parameter variations required to achieve the desired beam emittance and brightness. A similar study, covering a broader set of operating scenarios, has been reported for the CW photoinjector of LCLS-II [6].

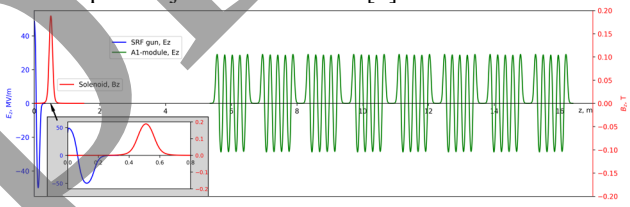

Figure 1: Electromagnetic field distribution along the SC photo injector.

Beam Dynamic Optimization in Injector

To evaluate the performance of the SC photo injector for future CW operation of the European XFEL the layout used in simulations is shown in Figure 1. The layout includes an L-band 1.6-cell SC cavity, an SC solenoid at z=0.5m, and, downstream, the first SC accelerating module (A1), whose first TESLA cavity is centered at z=6m; the setup is optimized to minimize emittance growth. The gun cavity peak field of 50 MV/m and a bunch charge of 100 pC were used as a reference, although lower gradients were also simulated to investigate the corresponding dilution of beam brightness. Thermal emittance of 0.5 μm/mm is used as estimate of expected copper cathodes emittance. The A1 module gradient was set to 29 MV/m, and its phase was fixed on-crest for the purpose of optimizing the photoinjector, with the goal of minimizing both projected and slice emittance at z=20 m. For start-to-end simulations, however, the A1 parameters were varied according to the three-stage bunch compression scheme. Considering the RF gradients achieved so far [7] and the separation of the solenoid from the gun cavity (in contrast to conventional normal-conducting photoinjector layouts), photocathode laser

†sumaira.zeeshan@desy.de

pulse shaping plays an even more significant role in determining the beam brightness.

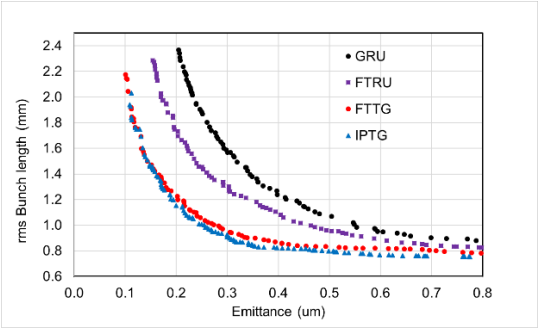

Figure 2: Results of the MOGA optimization for 50MV/m and four photocathode laser pulse shapes.

Photoinjector Optimization

The photoinjector parameters tuned during optimizations are, the gun phase, solenoid current, photocathode laser pulse duration, and transverse spot size. The general layout specifically the positions of the solenoid and the first accelerating module (A1) relative to the gun cavity was kept fixed after being optimized for the best performing configuration (FTTG). The results of the multiobjective genetic algorithm (MOGA [8] driving ASTRA code [9]) optimization for a gun gradient of 50 MV/m and the four photocathode laser pulse shapes described above are shown in Figure 2. The results are presented as a Pareto front in the plane of rms bunch length versus projected transverse emittance. Under these conditions, a minimum projected emittance of ~ 0.1 mm mrad can be achieved using advanced laser pulse shaping for electron bunch lengths of about 2 mm.

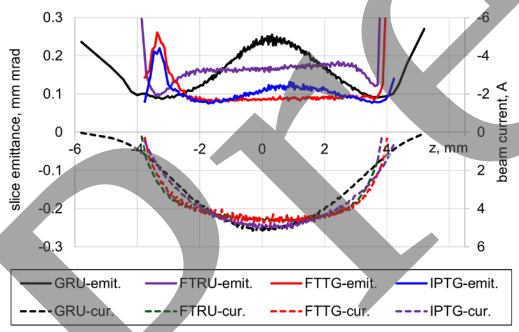

Figure 3: Slice emittance and beam current for 2 mm electron bunch length.

The FTRU case lies between the best (FTTG) and the baseline (GRU) configurations, although it is somewhat closer to the later. The reason for being away from the FTTG case could be the emittance compensation matching point, which for fully optimized setup would require to occur upstream of the A1 entrance, however due to the fixed layout the matching was constrained to the A1 entrance resulting in emittance minimum is slightly higher than the absolute minimum achievable. Nevertheless this need detailed further investigations. The transverse slice emittance, and beam current profiles along the bunch for the all photocathode laser pulse shapes for 2 mm rms bunch lengths are shown in the Figure 3. The charge distribution within the electron bunch is highest for Gaussian and lowest for Flattop and central slice emittance is lowest for the flattop and highest for the Gaussian.

Start to End Simulations

To evaluate the performance of the CW photoinjector and to assess the impact of photocathode laser pulse shaping on the final beam brightness at the undulator entrance, comprehensive start-to-end (S2E) simulations were performed for these four laser pulse shapes. The injector optimized parameter sets for all configurations, were subsequently tracked through the European XFEL beamline.

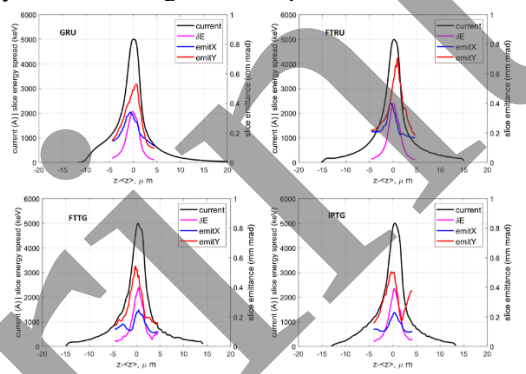

Figure 4: Current profiles, slice transverse normalized emittances and slice energy spread at the XFEL undulator entrance for four laser pulse shapes

The primary optimization objective at the XFEL entrance was to maximize the beam brightness B ~ $I_{beam}/(\varepsilon x \cdot \varepsilon y)$ at the end of the linac, as this directly translates into improved FEL performance. Beam transport was simulated using the Ocelot code [10], including collective effects such as space charge, wakefields, and coherent synchrotron radiation.

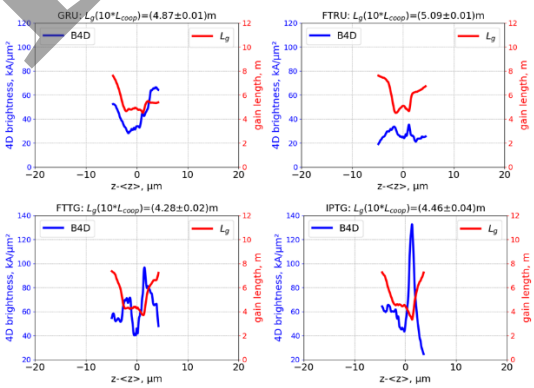

Figure 5: Local brightness and gain length distributions at the XFEL undulator entrance for four laser pulse shapes

The photo injector optimization at z = 20 m provided the input for the s2e simulations, with the ASTRA beam monitors at z = 5.23 m defining the initial beam, while the A1module RF parameters were refined in the bunch compression optimization. The CW mode EuXFEL beamline features three bunch compressors BC0, BC1, and BC2 operating at beam energies of 130 MeV, 0.6 GeV, and 1.95 GeV, respectively, with a final beam energy of 8 GeV

assumed after the main linac (L3). Initial compression factors of 3 and 7 were applied in BC0 and BC1, respectively, whereas the compression factor in BC2 was tuned to achieve a final peak beam current of approximately 5 kA. The three-stage compression scheme was iteratively optimized by simultaneously adjusting the RF parameters of the linacs to obtain the desired longitudinal phase space characteristics. A final slice energy spread of approximately 2 MeV was achieved by tuning the laser heater in the injector section. This value was determined from microbunching instability studies and was applied consistently to all four cases [11] . Figure 4 shows the current profiles, slice emittances and slice energy spread at the undulator entrance while the corresponding final beam parameters are summarized in Table 1. Figure 5 shows the 4D brightness and gain lengths for the four cases. The table also list the percentage difference w.r.t. FTTG in terms of emittance and brightness both after the injector and at undulator entrance. It can be inferred that IPTG performs better in the S2E simulations as compared to the injector. The brightness becomes 99% of the reference case as compared to 84% in the injector section. GRU also shows similar behaviour. However, the FTRU case showed degraded behaviour in the S2E simulations and needs further investigation.

Table 1: Photocathode (PC) Laser & Electron Beam Parameters With FTTG Case as the Reference

	Parameter	Unit	GRU	FTRU	**FTTG**	IPTG
PC laser	FWHM	ps	18.5	24.9	**25.7**	22.9
	BSA	mm	0.72	0.8	**0.69**	0.66
	σ_{xy}	mm	0.18	0.2	**0.22**	0.18
After photo injector (z = 20 m)	σ_t	mm	2.12	2	**2.02**	1.97
	$\varepsilon_{Proj\ xy}$	mmmrad	0.226	0.171	**0.113**	0.123
	w.r.t. ref	–	200%	152%	**100%**	109%
	$\varepsilon_{Avg\ xy}$	mmmrad	0.171	0.161	**0.097**	0.103
	w.r.t. ref	–	175%	165%	**100%**	106%
	$B_{4D\ avg}$	A/µm	131	159.2	**461**	389.1
	w.r.t.ref	–	28%	35%	**100%**	84%
Undulator entrance	I_{peak}	kA	5	5	**5**	5
	σ_t	µm	4.5	4.7	**4.6**	4.1
	$\pm\sigma z\ \varepsilon_{x\ avg}$	mmmrad	0.249	0.271	**0.167**	0.158
	w.r.t. ref	–	149%	162%	**100%**	95%
	$\pm\sigma z\ \varepsilon_{Y\ avg}$	mmmrad	0.362	0.434	**0.331**	0.349
	w.r.t. ref	–	109%	131%	**100%**	105%
	$\pm\sigma z.\ B_{4D\ avg}$	kA/µm	44.1	26.7	**63**	62.4
	w.r.t. ref	–	70%	42%	**100%**	99%
	Gain Length-	m	4.87	5.09	**4.28**	4.46
	w.r.t. ref	–	114%	119%	**100%**	104%

Photo Injector Performance Versus Gun Gradient

To estimate the performance degradation at reduced RF gradients as compared to 50 MV/m in the event if the target gradient cannot be achieved, studies were carried out for all considered photocathode laser pulse shapes. An optimization of the photoinjector was carried out for gun gradients of 45, 40, and 35 MV/m, while keeping the bunch charge fixed at 100 pC. Table 2 summarizes the main outcomes of this optimization study. Assuming an acceptable projected emittance of 0.25 mm mrad from the photoinjector, one can conclude that the desired performance can still be expected at reduced gun gradients even 35 MV/m for the FTTG and IPTG cases, greater than 40 for the FTRU and 48 MV/m for the GRU case. However, the brightness numbers degrade much faster for 35 MV/m for all cases. Figure 6 shows the corresponding emittance growth relative to the reference case (FTTG at 50 MV/m), as well as the average 4D brightness dilution indicated on the secondary (right) axis. Assuming an acceptable projected emittance of 0.25 mm mrad from the photoinjector, one can conclude that the desired performance can still be expected at reduced gun gradients even 35 MV/m for the FTTG and IPTG cases, greater than 40 for the FTRU and 48 MV/m for the GRU case. However, the brightness numbers degrade much faster for 35 MV/m for all cases.

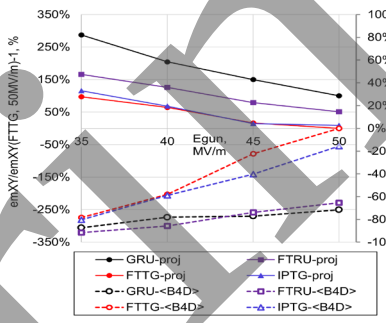

Figure 6: Electron beam performance at the photoinjector exit for various gun gradients.

Table 2: Electron Beam Parameters at the Photoinjector Exit (Z=20 M) for Various Gun Gradients

Parameter	Pulse Shape	35 MV/m	40 MV/m	45 MV/m	50 MV/m
Proj trans emit (mm mrad)	GRU	0.438	0.344	0.282	0.226
	FTRU	0.3	0.256	0.202	0.171
	FTTG	0.223	0.185	0.131	0.113
	IPTG	0.243	0.19	0.13	0.114
Avg slice emit (mm mrad)	GRU	0.372	0.288	0.216	0.179
	FTRU	0.263	0.199	0.195	0.161
	FTTG	0.201	0.15	0.112	0.097
	IPTG	0.227	0.155	0.124	0.103
Avg 4D brightness (kA/µm2)	GRU	57.9	100.7	105	131
	FTRU	38.7	65.5	121	159.2
	FTTG	99.82	193.8	357.6	461
	IPTG	91	189.4	275.5	389.1

SUMMARY

Simulations studies for the optimization of emittance and brightness in CW SRF gun of EuXFEL carried out for four photoinjector laser shapes and FTTG and IPTG profiles provide the best overall performance, achieving low projected emittance and high brightness at the injector exit. Start-to-end simulations through the full linac and three stage bunch compression confirm that these optimized injector parameters are largely preserved at the undulator entrance, directly improving FEL gain. The role of the gun gradient was numerically studied, qualifying options if the target parameters are not achieved. Both FTTG and IPTG can work at lower gradient and provide acceptable emittance and brightness values. The degradation behavior of FTRU case in S2E simulations needs further studies.

REFERENCES

[1] M. Altarelli, "The European X-ray free-electron laser facility in Hamburg," *NIMB*, vol. 269, p. 2845-2489, 2011. doi:10.1016/j.nimb.2011.04.034

[2] B. Faatz *et al.*, "Simultaneous operation of two soft x-ray free-electron lasers driven by one linear accelerator," *New Journal of Physics*, vol. 18, p. 062002, 2016. doi:10.1088/1367-2630/18/6/062002

[3] R. Brinkmann, et.al., "Prospects for CW operation of the European XFEL hard x-ray regime", in Proc. Free Electron Laser (FEL2014), Basel, Switzerland, MOP067 ISBN 978-3-95450-133-5, pp 210-214.

[4] R. Xiang et al., "Superconducting radio frequency photoinjectors for CW-XFEL," *Front. Phys.*, vol. 11, Apr. 2023. doi:10.3389/fphy.2023.1166179

[5] D. Bazyl, et.al., "CW Operation of the European XFEL: SC-Gun Injector Optimization, S2E Calculations and SASE Performance", DESY Hamburg 21-138 arXiv:2111.01756 November 2021 ISSN 0418-9833

[6] Z. Zhang et al., "Fault-tolerance analysis for an injector of continuous-wave free-electron lasers", *Phys. Rev. Accel. Beams*, vol. 28, no. 9, Sep. 2025. doi:10.1103/zz4w-tvxt

[7] E. Vogel et.al., "High gradients at SRF photoinjector cavities with low RRR copper cathode plug screwed to the cavity back wall", Oct 2023. https://arxiv.org/pdf/2310.02974

[8] J. Blank and K. Deb, pymoo: Multi-Objective Optimization in Python, in IEEE Access, vol. 8, pp. 89497-89509, 2020. doi:10.1109/ACCESS.2020.2990567

[9] K. Flottmann, ASTRA particle tracking code, http://www.desy.de/~mpyflo

[10] Ocelot Gateway, https://ocelot.readthedocs.io/en/latest/index.html

[11] I. Zagorodnov, and M. Dohlus., "Semianalytical Modeling of Multistage Bunch Compression with Collective Effects", *Phys. Rev. Spec. Top. Accel Beams*, vol. 14, no. 1, Jan. 2011. doi:10.1103/PhysRevSTAB.14.014403